ORIGINAL ARTICLE

lajss.org© Latin American Journal of Solids and Structures

www.lajss.org

Reliability of RC cross-sections designed for simple bending according to the 2014 and 2023 versions of NBR 6118 code

Gabriel Martinez Machado[a]*, Américo Campos Filho[a], Mauro de Vasconcellos Real[a]

[a]Universidade Federal do Rio Grande do Sul - UFRGS, Porto Alegre, RS, Brasil. E-mails: gabrielmachado@furg.br, mvrealgm@gmail.com, americo@ufrgs.br

* Corresponding author

https://doi.org/10.1590/1679-7825/e8343

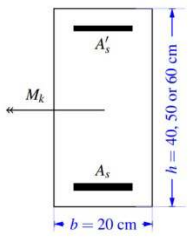
Abstract

This article presents a comparative study of the reliability of reinforced concrete (RC) cross-sections subjected to simple bending, designed at the ultimate limit state and following the recommendations of the 2014 and 2023 versions of the Brazilian code NBR 6118. The analyses are based on reliability theory by implementing the FORM algorithm on three rectangular cross-section configurations, considering three constant values of dimensionless bending moments and five different concrete strength classes between C30 and C90. Although the elements designed by NBR 6118:2023 have shown additions of up to 19% in the total steel cross-section area as a consequence of the implementation of the strength reduction factor (η_c), the results show no significant improvements in reliability compared to the 2014 previous version of NBR 6118.

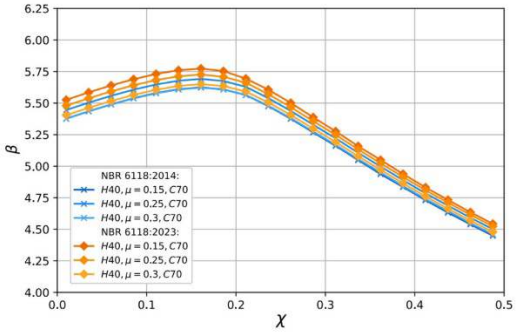
Keywords

reliability, simple bending, reinforced concrete, NBR 6118:2023, FORM

Graphical Abstract



Simulated cross-sections



Reliability indices for 40 cm height C-S (f_{ck}=70 MPa) – comparison between versions of NBR 6118 (2014 and 2023)

Cross-section	$\frac{A_{s,total\ (2023)}}{A_{s,total\ (2014)}}$	$\frac{\beta_{max\ (2023)}}{\beta_{max\ (2014)}}$
H40, μ = 0.15, C50	1.008	1.010
H40, μ = 0.15, C70	1.021	1.026
H40, μ = 0.15, C90	1.032	1.041
H40, μ = 0.25, C50	1.017	1.019
H40, μ = 0.25, C70	1.149	1.006
H40, μ = 0.25, C90	1.193	1.003
H40, μ = 0.30, C50	1.038	1.006
H40, μ = 0.30, C70	1.109	1.005
H40, μ = 0.30, C90	1.142	1.003

Design and Reliability variations for the 40cm height C-S

1 INTRODUCTION

The design of concrete structures has undergone constant and significant evolution over time, directly related to the techniques, materials, and design procedures. Nine years after the promulgation of the Brazilian code NBR 6118:2014 (ABNT, 2014), it has become necessary to promote a comprehensive review to update the design criteria and safety standards in line with the demands and experiences acquired during this period.

In this context, the revision of NBR 6118, presented in 2023 (ABNT, 2023), introduced some critical changes, reflecting the standard's current level of consolidation and maturity. The previous version, NBR 6118:2014, adopted the

Received: ago. 20, 2024. In revised form: out. 30, 2024. Accepted: nov. 03, 2024, Available online: nov. 04, 2024.
https://doi.org/10.1590/1679-7825/e8343

Latin American Journal of Solids and Structures. ISSN 1679-7825. Copyright © 2025. This is an Open Access article distributed under the terms of the Creative Commons Attribution License, which permits unrestricted use, distribution, and reproduction in any medium, provided the original work is properly cited.

exact recommendations of Eurocode 2 (CEN, 2004) regarding the criteria for concrete strength in the Ultimate Limit State (ULS) in bending with or without compression. However, the updated Eurocode 2 (2023) introduced a strength reduction factor (η_c) aimed at reducing the level of stresses in elements with characteristic compressive strength (f_{ck}) above 40 MPa. On the other hand, so that the results were not too conservative, a constant value of 3.5 ‰ was established for the ultimate strain of the concrete, regardless of the characteristic value of the concrete's compressive strength.

In comparison, the updates to NBR 6118:2023 were more conservative in this aspect, merely incorporating the strength reduction factor, η_c, into the previous assumptions based on Eurocode 2 (2004). This point has led to discussions regarding potential inconsistencies between the models, as the ultimate concrete strain remains unchanged in the current Brazilian standard. This divergence raises concerns about compatibility between the two normative frameworks, particularly in relation to high-strength concrete behavior.

In addition, the assessment and study of reliability applied to reinforced concrete (RC) structures have been highly explored over the last five decades. Specifically regarding the Brazilian experience in this context, many studies have been conducted to clarify and deepen the research on the safety of reinforced concrete elements designed according to the Brazilian codes. In this regard, it is worth highlighting works such as the one by Stucchi and Santos (2007), who conducted a comparative reliability assessment of beams and slabs designed according to NBR 6118 (2014) and ACI 318-05. Concerning the reliability of reinforced concrete beams works by Scherer et al. (2021) and Santos et al. (2014) can also be mentioned, with the latter extending to steel and composite steel-concrete beams. Finally, the recent contributions of Santiago et al. (2019), who proposed the calibration of safety factors in the Brazilian standard based on reliability, and Pires and Gomes (2024), who evaluated the reliability of simply supported beams under fire conditions, should also be highlighted.

However, due to the updating of NBR 6118:2023, there is a need to assess the impacts produced by this version of the code on the design and reliability of structures. More recently, studies, such as those presented by Borges (2023) and Schuler (2023), have evaluated the impact of the introduction of the η_c coefficient on the design of columns simultaneously subjected to axial compression and biaxial bending. Regarding reliability, the impacts caused by adding this and other parameters are still unknown or poorly explored.

Therefore, this study aims to develop analyses to assess the changes brought about by the 2023 version of the Brazilian code regarding the total steel cross-section area ($A_s + A_s'$) and rectangular reinforced concrete cross-section reliability index (β) in simple bending at the ultimate limit state. For this purpose, it was necessary to employ a numerical computational model capable of estimating the actual flexural capacity of the cross-sections through mean resistance parameters based on the mechanical model presented in the *fib* Model Code 2010 (2013). The reliability of the sections must then be estimated by the numerical application of the First-Order Reliability Method (FORM) via the improved Hasofer-Lind and Rackwitz-Fiessler algorithm (iHLRF).

2 DESIGN OF REINFORCED CONCRETE CROSS-SECTIONS TO NORMAL LOADS

Initially, to establish the necessary conditions for the proposed studies, a survey of the normative criteria associated with the design and verification of reinforced concrete sections by the Brazilian code should be carried out. Therefore, sections 2.1 and 2.2 present, respectively, the main parameters and recommendations of the NBR 6118:2014 version and the subsequent changes promoted by the 2023 update.

2.1 NBR 6118:2014 recommendations

The NBR 6118 guidelines for designing reinforced concrete elements range from definitions of material properties, the behavior of stress-strain diagrams for steel and concrete, the establishment of partial safety factors, and other criteria for determining the elements' resistance stresses and possible strain distributions.

2.1.1 Concrete stress-strain diagram

Item 8.2.10.1 of NBR 6118:2014 defines the criteria for the behavior of the idealized stress-strain diagram for concrete under compression at the ultimate limit state (ULS) (Figure 1). There are two distinct sections: the first is defined by a curve (equation in the image) and then a straight line of constant stress, limited to 85% of the design compressive strength.

The compressive strains of the concrete, ε_{c2} and ε_{cu} vary according to the strength class of the concrete. Equations 1 and 2 correspond to the values for elements with $f_{ck} \leq 50$ MPa, while Equations 2 and 3 are used for values of f_{ck} greater than 50 MPa.

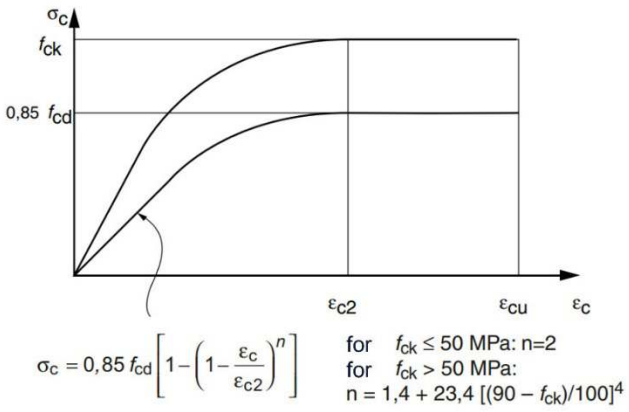


Figure 1 Idealized stress-strain diagram of concrete - NBR 6118:2014.

$$\varepsilon_{c2} = 2‰ \ (f_{ck} \leq 50 \text{ MPa}) \tag{1}$$

$$\varepsilon_{cu} = 3.5‰ \ (f_{ck} > 50 \text{ MPa}) \tag{2}$$

$$\varepsilon_{c2} = 2.0‰ + 0.085‰ \cdot (f_{ck} - 50)^{0.53} \ (f_{ck} \leq 50 \text{ MPa}) \tag{3}$$

$$\varepsilon_{cu} = 2.6‰ + 35‰ \cdot [(90 - f_{ck})/100]^4 \ (f_{ck} > 50 \text{ MPa}) \tag{4}$$

2.1.2 Stress-strain diagram of reinforcement steel

Regarding the stress-strain diagram of reinforcing steel, section 8.3.6 of the Brazilian code allows ideal elastoplastic behavior to be considered using the simplified bi-linear model in Figure 2, up to a strain limit of 10‰. The slope of the upward section, defined as the elastic modulus of the steel (E_s), corresponds to 210 GPa.

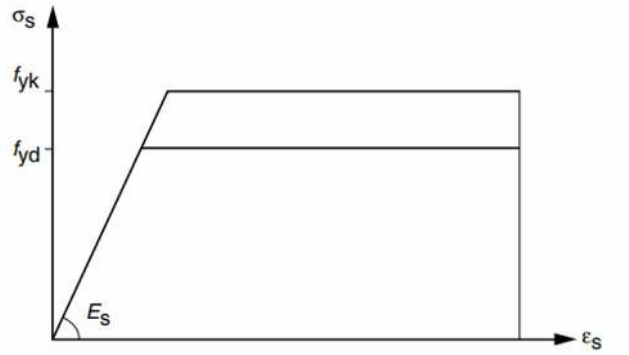


Figure 2 Stress-strain diagram of reinforcing steels - NBR 6118:2014.

2.1.3 Combination of actions

NBR 6118:2014 divides the ultimate combinations of actions (ELU) into the following categories: normal/special or construction combinations (Equation 5) and exceptional ultimate combinations (Equation 6), both shown below.

$$F_d = \gamma_g F_{gk} + \gamma_{\varepsilon g} F_{\varepsilon gk} + \gamma_q \left(F_{q1k} + \sum \psi_{0j} F_{qjk}\right) + \gamma_{\varepsilon q} \psi_{0\varepsilon} F_{\varepsilon qk} \tag{5}$$

$$F_d = \gamma_g F_{gk} + \gamma_{\varepsilon g} F_{\varepsilon gk} + F_{q1exc} + \gamma_q \sum \psi_{0j} F_{qjk} + \gamma_{\varepsilon q} \psi_{0\varepsilon} F_{\varepsilon qk} \tag{6}$$

Where F_d is the design action for the ultimate combination; F_{gk} represents direct permanent actions; $F_{\varepsilon k}$ represents permanent indirect ($F_{\varepsilon gk}$) and variable ($F_{\varepsilon qk}$) actions, F_{qk} represents the direct variable actions of which F_{q1k} is considered the main one.

The terms γ_g, $\gamma_{\varepsilon g}$, γ_q, and $\gamma_{\varepsilon q}$ are the partial factors for actions. For normal combinations of general actions that are unfavorable to safety, a value of 1.4 is recommended.

The partial factors for minimizing direct or indirect variable actions, considered secondary, ψ_{0j} and $\psi_{0\varepsilon}$, are set at 0.50 for variable loads on residential buildings, 0.70 for commercial buildings, and 0.60 for wind or temperature actions.

2.1.4 Resistance reduction factors

To determine the design strengths of concrete and steel, γ_c and γ_s factors are implemented to reduce the characteristic strengths ($f_{cd}=f_{ck}/\gamma_c$ and $f_{yd}=f_{yk}/\gamma_s$). Table 1 shows the values of these factors as recommended by NBR 6118:2014.

Table 1 Values of γ_c and γ_s (NBR 6118:2014)

Combination	Concrete (γ_c)	Steel (γ_s)
Normal	1.4	1.15
Special or construction	1.2	1.15
Rare	1.2	1.0

2.1.5 Parameters for bending design

A simplification in the design of bending cross-sections allowed by the Brazilian code uses a rectangular stress diagram instead of the idealized diagram in Figure 1. In this case, the stresses in the cross-section occur up to the depth $y = \lambda x$, where:

$$\lambda = 0.8 \ (f_{ck} \leq 50 \text{ MPa}) \tag{7}$$

$$\lambda = 0.8 - (f_{ck} - 50)/400 \ (f_{ck} > 50 \text{ MPa}) \tag{8}$$

The concrete stress for constant-width sections will be determined as $\sigma_{cd}=\alpha_c f_{cd}$, where α_c can be defined for this particular case as described in Equations 9 and 10.

$$\alpha_c = 0.85 \ (f_{ck} \leq 50 \text{ MPa}) \tag{9}$$

$$\alpha_c = 0.85[1.0 - (f_{ck} - 50)/200] \ (f_{ck} > 50 \text{ MPa}) \tag{10}$$

The cross-sections are then designed for the stress equilibrium condition of strain distributions denoted by 2 and 3 (ductile rupture condition), as shown in Figure 3. In this case, the code sets a limit on the relative height of the neutral axis ($\xi = x/d$) of 0.45 for elements with $f_{ck} \leq 50$ MPa and 0.35 if $f_{ck} > 50$ MPa, for cross-sections without redistribution.

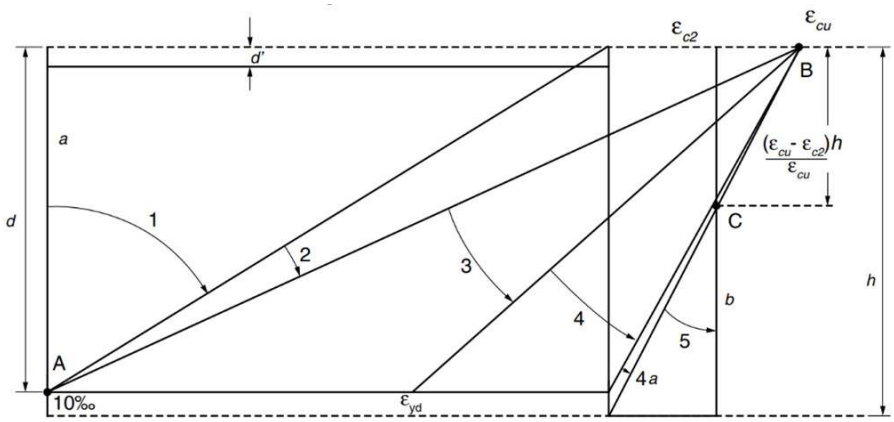


Figure 3 Strain domains for cross-sections at the ULS (NBR 6118:2014).

Also, as a way of avoiding the fragile rupture of cross-sections, item 17.3.5 of NBR 6118:2014 establishes that the reinforcement must be checked for a minimum moment equivalent to the rupture moment of a plain concrete cross-section, respecting the absolute minimum steel ratio of 0.15%. This moment is converted into a minimum steel area according to Equation 11 (Araújo, 2014), calculated as a function of the mean tensile strength of the concrete (f_{ctm}).

$$A_{s,min} = 0.26\, bhf_{ctm}/f_{yd} \geq 0.15\%bh \tag{11}$$

The design equations for simple bending can be deduced from balancing forces and moments. Equations 12 and 13 correspond to the formulas for calculating the dimensionless variables for moment and neutral axis position, respectively.

$$\mu = \frac{M_d}{bd^2\sigma_{cd}} \tag{12}$$

$$\xi = \frac{1-\sqrt{1-2\mu}}{\lambda} \tag{13}$$

Where M_d is the design bending moment, b and h correspond to the width and height of the cross-section, and d is the effective depth. The limit values for the dimensionless bending moment (μ_{lim}) are calculated from the limit values of ξ (Equation 14).

$$\mu_{lim} = \lambda\xi_{lim}(1 - 0.5\lambda\xi_{lim}) \tag{14}$$

When $\mu \leq \mu_{lim}$, the beam corresponds to a simply reinforced beam. Equation 15 provides the formula for determining the cross-sectional steel area for these cases.

$$A_s = \lambda\xi bd\frac{\sigma_{cd}}{f_{yd}} \tag{15}$$

However, when $\mu > \mu_{lim}$, the beam must contain reinforcement placed in the compression region and is called a doubly reinforced beam. The calculations of the bottom and top reinforcement of the cross-section (A_s and $A_s^{'}$) are shown in Equations 16 and 17 (Araújo, 2014), where σ_{sd} is the design steel stress and $M_{d,lim}$ is the limit design bending moment when $\mu = \mu_{lim}$.

$$A_s = \lambda\xi bd\frac{\sigma_{cd}}{f_{yd}} \tag{16}$$

$$A_s = (A'_s\sigma'_{sd} + \lambda\xi_{lim}bd\sigma_{cd})/f_{yd} \tag{17}$$

2.2 NBR 6118:2023 changes in the design of cross-sections

Regarding the design of cross-sections in flexure, the update of NBR 6118:2023 brought just a few changes compared to the 2014 version. The changes are mainly concentrated in the concrete stress-strain diagrams, which now include the strength reduction factor (η_c) as a tool to prevent sudden failure in concretes with higher compressive strength. This coefficient applies to elements with a characteristic compressive strength greater than 40 MPa, as shown in Figure 4.

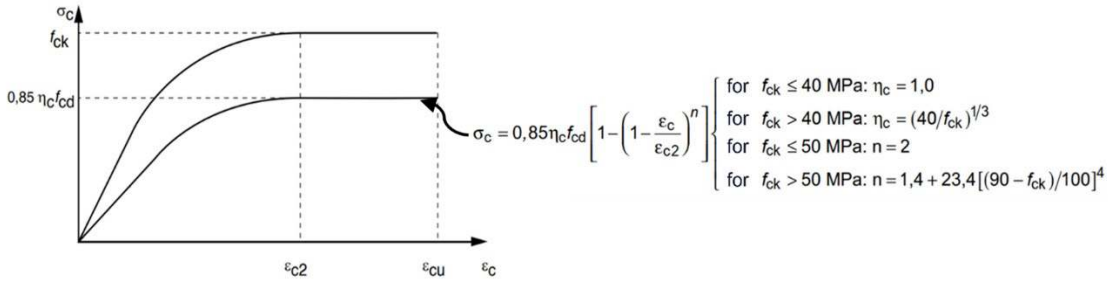


Figure 4 Idealized stress-strain diagram according to NBR 6118:2023.

In design, the use of the simplified rectangular diagram is still permitted. The information and equations presented in 2.1.5 remain valid, except for the value of the compressive stress, which is now calculated as $\sigma_{cd} = \alpha_c\, \eta_c\, f_{cd}$.

3 MECHANICAL DESIGN MODEL

3.1 Generalities

The analyses carried out in this work make it necessary to implement a numerical computer model that represents the actual behavior of the elements to determine the ultimate strength capacity. For this purpose, the recommendations of the *fib* Model Code 2010 (2013) are applied, using the average strength parameters of the materials.

Concrete behavior under uniaxial compression stresses in short-term load tests is represented by the diagram in Figure 5, whose stresses are determined using Equation 18.

$$\frac{\sigma_c}{f_{cm}} = -\left(\frac{k\cdot\eta-\eta^2}{1+(k-2)\cdot\eta}\right) \text{ for } |\varepsilon_c| < |\varepsilon_{c,lim}| \tag{18}$$

Where: $\eta = \varepsilon_c/\varepsilon_{c1}$; k is the plasticity number; ε_{c1} is the strain at the point of maximum stress and E_{c1} is the secant modulus between the origin and the peak stress.

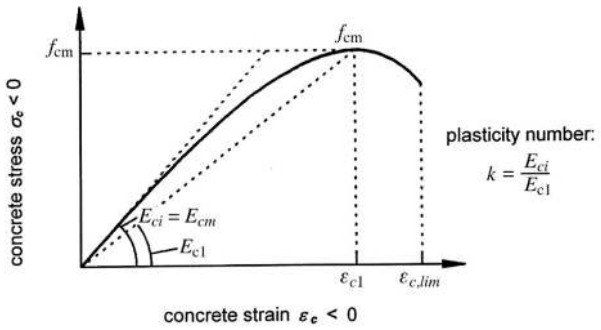


Figure 5 Stress-strain diagram for compressed concrete according to fib (2010).

In addition, the model presented by *fib* allows the contribution of the concrete tensile regions (σ_{ct}) to be considered when calculating the cross-section total strength. Figure 6 presents the stress-strain and stress-crack opening relations of concrete in tension.

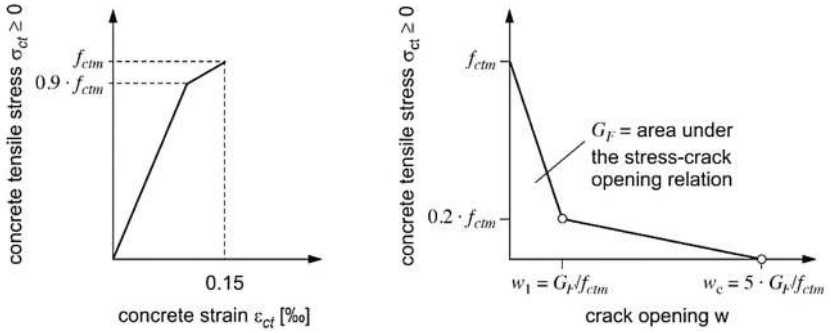


Figure 6 Representation of the stress-strain and stress-crack opening relations of concrete in tension (fib, 2010).

The formulations for determining the stresses in the sections of the stress-strain diagram are given by Equations 19 and 20.

$$\sigma_{ct} = E_{ci} \cdot \varepsilon_{ct} \text{ , for } \sigma_{ct} \leq 0{,}9 \cdot f_{ctm} \tag{19}$$

$$\sigma_{ct} = f_{ctm} \cdot \left(1 - 0.1\,\frac{0.15‰-\varepsilon_{ct}}{0.15‰-0.9f_{ctm}/E_{ci}}\right), \text{ for } 0.9f_{ctm} < \sigma_{ct} \leq f_{ctm} \tag{20}$$

Where ε_{ct} is the tensile strain and E_{ci} is the tangent modulus of elasticity of concrete.

For the consideration of the stresses due to the crack opening process in the resistance model, the diagram on the right side of Figure 6 might be used. In this case, the stresses for each linear segment shown in the diagram can be calculated using Equations 21 and 22, as a function of the crack-opening (w) in millimeters.

$$\sigma_{ct} = f_{ctm} \cdot \left(1.0 - 0.8\frac{w}{w_1}\right) \text{, for } w \leq w_1 \quad (21)$$

$$\sigma_{ct} = f_{ctm} \cdot \left(0.25 - 0.05\frac{w}{w_1}\right) \text{, for } w_1 < w \leq w_c \quad (22)$$

Where G_F is the fracture energy in N/mm. Thus, the stresses produced by the cracking process occur over a discontinuous region around the stabilized crack, with a total extension equal to $2l_{s,max}$. The $l_{s,max}$ length (Equation 23) is calculated as a function of the mean adhesion stress between the steel and concrete materials (τ_{bms}), the concrete cover (c), the diameter of the bars (φ_s), and the effective reinforcement ratio ($\rho_{s,ef}$).

$$l_{s,max} = k \cdot c + \frac{1}{4} \cdot \frac{f_{ctm}}{\tau_{bms}} \cdot \frac{\varphi_s}{\rho_{s,ef}} \quad (23)$$

That said, it becomes possible to establish a direct relationship between stresses and strains caused by the crack-opening process (ε_{wj}) and the resulting stabilization process over this discontinuous region, where $\varepsilon_{wj}=w_j/\left(2l_{s,max}\right)$.

On the other hand, the same ideal elastoplastic behavior shown in Figure 2 is assumed to calculate the steel stresses. The model is valid for both compressive and tensile stresses, where the maximum stress acting on the material is the yield stress (f_y), up to the maximum stretching strain of the rebars equal to 50‰ (*fib,* 2010).

The algorithm for the computational implementation of this model was then developed in the Python language through an iterative process that aims to find the actual neutral axis position (x) and implements Green's theorem to integrate the stress regions of any polygonal section, so the proportionality factor Δ can be minimized until the equilibrium condition of Equation 24 is satisfied.

$$f(x, \Delta) = \delta M_x = \Delta \cdot M_{Rx} - M_{Ax} \quad (24)$$

Therefore, by knowing the applied moment (M_{Ax}) in the cross-section and then integrating the stress regions shown above, the maximum bending resistant moment of the section (M_{Rx}) is finally determined. The dashed lines indicate the separation among stress integration regions in Figure 7.

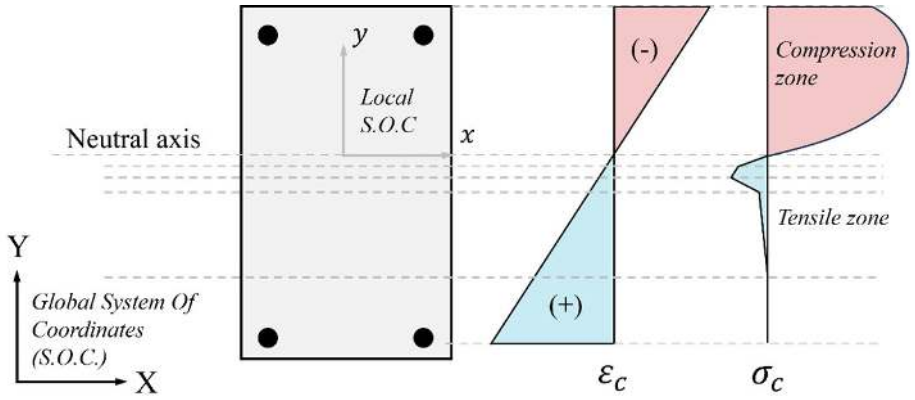


Figure 7 Concrete stress regions considered in the mechanical model.

3.2 Numerical model validation

The model was validated using a test database of 53 reinforced concrete beams with flexural failure, taken from the following references: Janney et al. (1956), Bresler and Scordelis (1963), Base and Read (1965), Kong and Rangan (1998), Garcia (2018), Prieto Rabade and Tanner (2008), Arezoumandi et al. (2015), Ning et al. (2015), Canaval (2016) and Kulkarni and Shah (1998). The ratios between the actual experimental moments and the calculated moments were determined to enable the application of the Kolmogorov-Smirnov (K-S) and the Chi-squared (χ^2) adherence tests and the fitting of an appropriate statistical distribution. The K-S test evaluates the absolute maximum distance between the cumulative distribution function of the observed data and the theoretical distribution under analysis. On the other hand, the χ^2 test assesses the probability of adherence between the frequencies shown in the data histogram and those from the fitted distribution.

As detailed in Machado (2024), the Gaussian (normal) distribution model showed the best indicators for the problem dataset, with sample mean μ = 1.01, standard deviation σ = 0.07, and coefficient of variation of the resistance model $C.O.V_{res}$ = 0.07. The probability density function for the Gaussian distribution is shown in Figure 8.

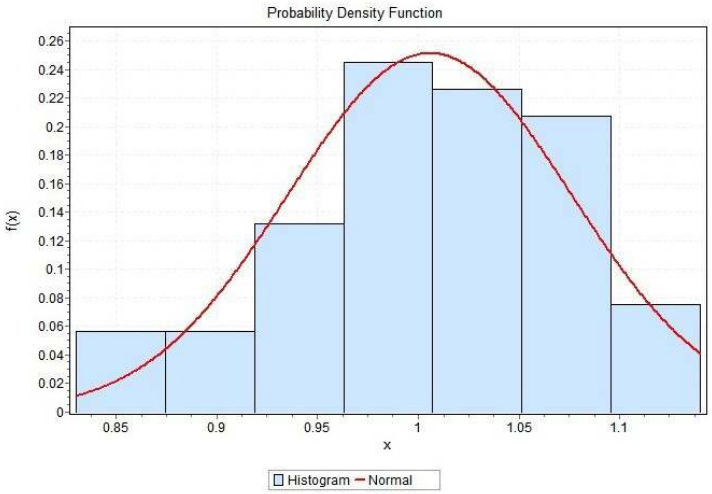


Figure 8 Data fitting to Gaussian (normal) distribution.

To be discussed below, reliability analyses require the definition of the model's average coefficient of variation ($C.O.V_m$), as explained by Nowak and Szerszen (2003) and Ribeiro et al. (2021), which must take into account test uncertainties and inaccuracies ($C.O.V_{test}$) and other resistance and geometry variabilities ($C.O.V_{spec}$) and can be estimated at approximately 4% each. The determination of $C.O.V_m$ is given by Equation 25 and results in $C.O.V_m$ = 0.041.

$$COV_m = \sqrt{COV_{res}^2 - COV_{test}^2 - COV_{spec}^2} = \sqrt{0.07^2 - 0.04^2 - 0.04^2} = 0.041 \tag{25}$$

4 STRUCTURAL RELIABILITY

According to Melchers and Beck (2018), structural reliability is a tool to measure the degree of certainty of a system (or element) in meeting its specifications, operating conditions, and design lifespan concerning the intrinsic uncertainties caused by model simplifications, as well as by physical, mechanical and geometric property variations, external actions, human errors, among others.

4.1 Performance function

As discussed by Ang and Tang (2006), the problem of reliability in engineering systems essentially consists of a capacity (resistance) versus demand (loading) problem. In this way, it is important to define a performance function that characterizes the failure mode of the studied problem to allow the evaluation of the failure conditions. This performance function is generally described as in Equation 26, where X is the random variables vector ($X = \{X_1, X_2, X_3, \ldots\}$).

$$g(X) = g(X_1, X_2, X_3, \ldots, X_n) \tag{26}$$

The performance function can be particularized in structural reliability analyses according to the safety margin concept, represented in Equation 27 below.

$$g(R, S) = R - S \tag{27}$$

In this equation, R consists of the resistance variable vector of the structural system, and S is the set of external actions that affect the structure. It is clear, therefore, that establishing the condition R-$S > 0$ with a certain safety margin is of interest since the complementary condition (R-$S < 0$) represents the status of structural failure.

The probability of failure becomes one of the unknowns of interest in structural reliability analysis. In the case of normal and statistically independent random variables, the probability of failure (P_f) is directly related to the mean (μ_M,

Equation 29) and standard deviation (σ_M, Equation 30) of the safety margin M by a cumulative standard normal distribution function Φ as indicated in Equation 28.

$$P_f = \Phi\left({}^{-\mu_M}/_{\sigma_M}\right) = \Phi(-\beta) \tag{28}$$

$$\mu_M = \mu_R - \mu_S \tag{29}$$

$$\sigma_M = \sqrt{\sigma_R^2 + \sigma_S^2} \tag{30}$$

As shown in Equation 28, the probability of failure can then be defined by a β parameter, known as the reliability index, which is extensively used in engineering problems to measure the safety level of a structure.

4.2 The FORM and the reliability index

According to Haldar and Mahadevan (2000), solving the probability of failure equation for problems in which the performance function is not simple is rarely feasible. Therefore, approximate methods with numerical or statistical approaches have been widely disseminated as a tool for determining the reliability index (β), formally described as a safety assessment parameter that represents the distance between the average value of the safety margin and the point of failure.

In this context, the First Order Reliability Method, FORM, is a numerical technique that simplifies calculation processes by approximating the performance function through a Taylor series expansion. The process allows the probability of failure of problems to be estimated, even for correlated input variables that may not present a normal distribution.

This is done through a composite transformation, which transforms the original variables' vector X_i (from the physical space) into equivalent Z_i correlated standardized normal variables and, finally, into the Y_i non-correlated variables vector of to the standard normal space. To do this, it is necessary to modify the reliability index calculation so that the limit state equation can be solved from a specific design point. The variables vector X_i is now expressed as shown below (Equation 31), where the superscripted N refers to the equivalent normal distribution.

$$X_i = \mu_{X_i}^N + Y_i \sigma_{X_i}^N \tag{31}$$

In standard normal space, the β index will have the geometric meaning represented by Figure 9, corresponding to the minor geometric distance between the origin of the standard space and the failure surface at a “design point” ($\boldsymbol{y}^*$), as defined in Equation 32.

$$\beta = \left|\left|\boldsymbol{y}^*\right|\right| = \sqrt{Y^{*T} Y^*} \tag{32}$$

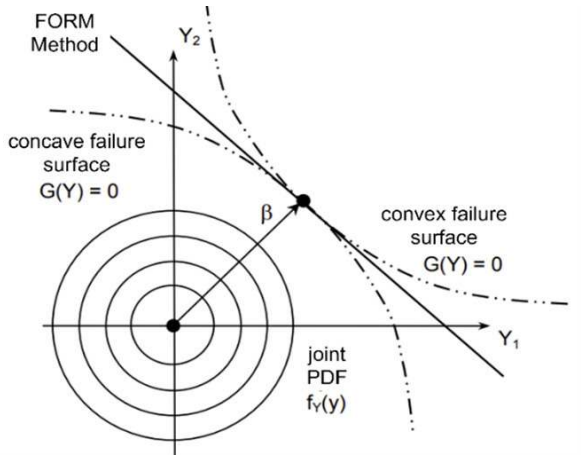


Figure 9 Approximation process of the FORM and the reliability index (adapted from Lopes (2007)).

This process is carried out iteratively so that minimizing the distance between the origin of the reduced space and the limit state function at a point y_{k+1} is achieved by applying some optimization algorithms, such as Hasofer-Lind and Rackwitz-Fiessler algorithm (HLRF) or improved Hasofer-Lind and Rackwitz-Fiessler algorithm (iHLRF).

5 RELIABILITY ANALYSIS OF CROSS-SECTIONS IN SIMPLE BENDING

The cross-section of the analyzed beams will be rectangular, with a width b of 20 centimeters and a height h with dimensions of 40, 50, and 60 centimeters, as shown in Figure 10. The δ ratio (d'/d) will be constant at 0.10, so that the effective depths of the beams will be 36.2, 45.5, and 54.5 centimeters, respectively. As a standardization tool for comparative analyses, the beams were designed for specific values of dimensionless bending moment (μ), in the order of 0.15, 0.25, and 0.30, according to the design from NBR 6118:2014. Also, the simulations presented in the paper consider reinforced concrete elements composed of granite aggregate with characteristic compressive strength in five different configurations: 30, 40, 50, 70, and 90 MPa.

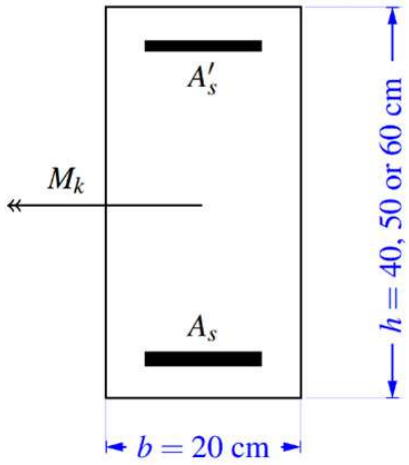


Figure 10 Cross-sections considered in this study.

Perfect elastoplastic behavior was assumed for CA-50 steel (f_{yk} = 500 MPa) when checking the cross-sections using the strength capacity estimation model. In terms of reliability analysis, a maximum tolerance of 1×10^{-3} was established for numerical inaccuracies between iterative processes through the computer implementation of the FORM via the iHRLF algorithm. Table 2 summarizes the probabilistic models used for the random variables considered in the analyses, which are all statistically independent. The referred models are intended to represent the reality of structures built in Brazil, as detailed in the following references: Santos et al. (2014), Santiago (2018), Coelho (2011), JCSS (2001a), JCSS (2001b) Stewart (1996) and Stucchi et al. (2011).

Table 2 Probabilistic models of the random variables

Variable	μ_x	σ_x	*COV.*	Distribution
Cross-section base (b - cm)	20 + 0.4	1.22	0.06	Gaussian
Cross-section height (h - cm)	50 + 0.16	2.56	0.045	Gaussian
Distance between bars G.C. and bottom of section (d' - cm)	d' + 0.2	0.045 (d' + 0.2)	0.045	Gaussian
Concrete compressive strength (f_c)*	(1.1 to 1.22) f_{ck}*	(0.1 to 0.18) f_{ck}*	0.09 to 0.15*	Gaussian
Steel yield strength (f_y)	1.22 f_{yk}	0.05 f_{yk}	0.04	Gaussian
Permanent actions (g)	g_k	0.1 μ_x	0.10	Gaussian
Variable actions (q)	0.93 q_k	0.2 μ_x	0.20	Gumbel
Resistance model uncertainties (θ_R)	1.01	0.041 μ_x	0.041	Gaussian
Load model uncertainties (θ_S)	1.00	0.05 μ_x	0.05	L.N.

* Variable parameters depending on the concrete strength class, according to Santiago (2018).

The reliability index β is calculated for a design point that satisfies the equilibrium condition of the limit state equation $g(X)$ (Equation 33) in which θ_R and θ_S represent the uncertainties of resistance and load models. In this case, the applied moment (M_s) is composed of moments due to permanent and variable actions, M_{Gk} and M_{Qk}, respectively, shown in Equations 34 and 35, where χ is the ratio between variable and total loads on the element.

$$g(X) = \theta_R M_R - \theta_S M_S = \theta_R M_R - \theta_S\left(M_{Gk} + M_{Qk}\right) \tag{33}$$

$$M_{Gk} = M_d/\left[\gamma_g + \gamma_q \cdot \left(\chi/(1-\chi)\right)\right] \quad (34)$$

$$M_{Qk} = M_d/\left[\gamma_q + \gamma_g \cdot \left((1-\chi)/\chi\right)\right] \quad (35)$$

Sections 5.1 and 5.2 below present the individual design results and the variations in the reliability index as a function of different χ ratios, for 20 points between 0 and 0.5, of the elements designed by the 2014 and 2023 versions of NBR 6118, respectively. In both cases, the partial factors for permanent and variable actions (γ_g and γ_q) are equal to 1.4, as well as the partial factors for concrete and reinforcing steel (γ_c and γ_s) are equal to 1.4 and 1.15. The design value of the modulus of elasticity of reinforcing steel (E_s) is assumed 210 GPa.

Next, Section 5.3 corresponds to a comparative evaluation of the obtained results.

5.1 Brazilian code NBR 6118:2014 design

This section presents the design and reliability results of the beams according to the criteria of NBR 6118:2014. Tables 3 to 5 show the bottom and top reinforcement steel areas (A_s and A_s') calculated for each cross-section, in cm^2. Figures 11 to 13 correspond to the variation graphs of the reliability indices as a function of χ, for cross-section heights of 40, 50, and 60 centimeters. The minimum reinforcement conditions and the neutral axis's limit depth were checked to maintain the elements' ideal ductility conditions. In cases where doubly reinforced concrete beams were required, the minimum steel area was set to 2 ϕ 6.3 mm, equivalent to 0.62 cm^2. Therefore, the design results of the three cross-sections are presented below. Once dimensioned, it is possible to present the dataset from the reliability analyses plotted in the following figures.

Table 3 Calculated reinforcement areas (A_s and A_s') for 40 centimeters height beams in accordance with NBR 6118:2014

Strength Classes	A_s	A_s'	A_s	A_s'	A_s	A_s'
	$\mu = 0.15$		$\mu = 0.25$		$\mu = 0.3$	
C30	4.95	-	8.88	-	11.08	0.62
C40	6.61	-	11.84	-	14.78	0.62
C50	8.26	-	14.81	-	18.47	0.62
C70	10.40	-	18.28	1.74	21.84	5.70
C90	11.89	-	20.68	3.24	24.75	7.86

Table 4 Calculated reinforcement areas (A_s and A_s') for 50 centimeters height beams in accordance with NBR 6118:2014

Strength Classes	A_s	A_s'	A_s	A_s'	A_s	A_s'
	$\mu = 0.15$		$\mu = 0.25$		$\mu = 0.3$	
C30	6.23	-	11.17	-	13.93	0.62
C40	8.30	-	14.89	-	18.57	0.62
C50	10.38	-	18.61	-	23.21	0.62
C70	13.08	-	22.97	2.12	27.41	6.95
C90	14.94	-	25.97	3.95	31.05	9.58

Table 5 Calculated reinforcement areas (A_s and A_s') for 60 centimeters height beams in accordance with NBR 6118:2014

Strength Classes	A_s	A_s'	A_s	A_s'	A_s	A_s'
	$\mu = 0.15$		$\mu = 0.25$		$\mu = 0.3$	
C30	7.46	-	13.37	-	16.68	0.62
C40	9.94	-	17.83	-	22.24	0.62
C50	12.43	-	22.29	-	27.80	0.62
C70	15.66	-	27.51	2.56	32.85	8.41
C90	17.90	-	31.12	4.78	37.21	11.59

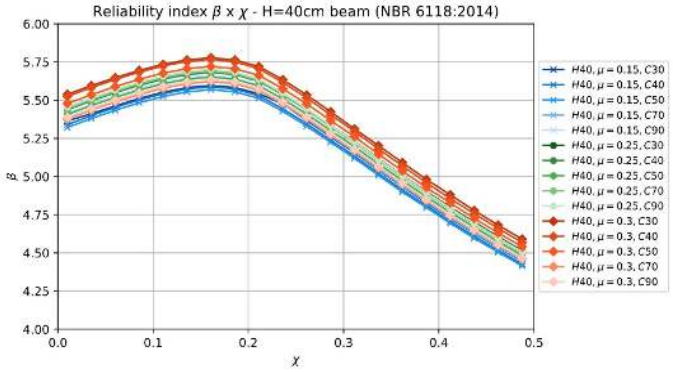


Figure 11 β x χ curves for 40 centimeters height beams designed in accordance with NBR 6118:2014.

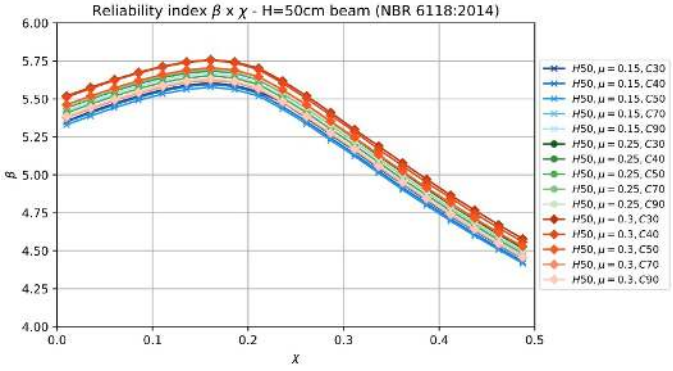


Figure 12 β x χ curves for 50 centimeters height beams designed in accordance with NBR 6118:2014.

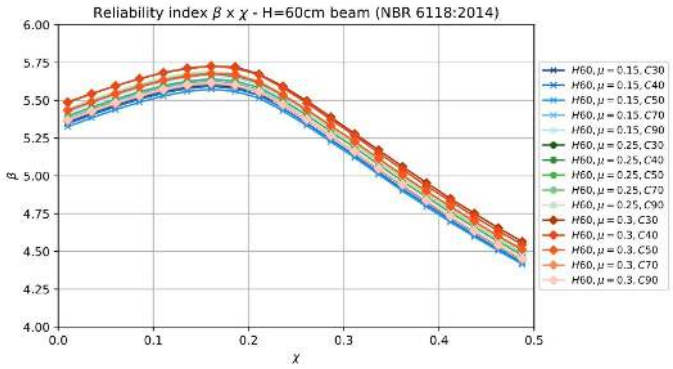


Figure 13 β x χ curves for 60 centimeters height beams designed in accordance with NBR 6118:2014.

The cross sections with different heights showed essentially the same behavior regarding the variation of the reliability index (β) as a function of the ratio of variable loads on the structure. The highest values of β occurred at approximately χ = 0.17. Therefore, reliability tends to decrease as the value of χ increases due to the rise in uncertainties associated with this type of action.

It can also be seen that the variations resulting from the increase in stresses (variation of μ), between different f_{ck} values, influenced the reliability index values by a maximum of 3%.

5.2 Brazilian code NBR 6118:2023 design

As presented in the previous section, the design and reliability results are shown below, this time for the elements designed according to NBR 6118:2023. Based on the information highlighted in 2.2, differences should be noted for elements with f_{ck} > 40 MPa, where the new strength reduction factor η_c is applied.

The elements were designed for the same values of characteristic moments, M_k, calculated by the 2014 version of the Brazilian code. Therefore, the original values of the dimensionless bending moments are only kept for identification and comparison purposes since the actual values of μ had to be updated.

Tables 6 to 8 below summarize the design results for the beams with the proposed cross-sections.

Table 6 Calculated reinforcement areas (A_s and A_s') for 40 centimeters height beams in accordance with NBR 6118:2023

Strength Classes	A_s	A_s'	A_s	A_s'	A_s	A_s'
	$\mu = 0.15$		$\mu = 0.25$		$\mu = 0.3$	
C30	4.95	-	8.88	-	11.08	0.62
C40	6.61	-	11.84	-	14.78	0.62
C50	8.32	-	15.05	-	18.36	1.47
C70	10.62	-	18.20	4.81	21.76	8.78
C90	12.28	-	20.60	7.95	24.67	12.58

Table 7 Calculated reinforcement areas (A_s and A_s') for 50 centimeters height beams in accordance with NBR 6118:2023

Strength Classes	A_s	A_s'	A_s	A_s'	A_s	A_s'
	$\mu = 0.15$		$\mu = 0.25$		$\mu = 0.3$	
C30	6.23	-	11.17	-	13.93	0.62
C40	8.30	-	14.89	-	18.57	0.62
C50	10.46	-	18.92	-	23.06	1.83
C70	13.35	-	22.84	5.87	27.28	10.69
C90	15.43	-	25.83	9.68	30.91	15.32

Table 8 Calculated reinforcement areas (A_s and A_s') for 60 centimeters height beams in accordance with NBR 6118:2023

Strength Classes	A_s	A_s'	A_s	A_s'	A_s	A_s'
	$\mu = 0.15$		$\mu = 0.25$		$\mu = 0.3$	
C30	7.46	-	13.37	-	16.68	0.62
C40	9.94	-	17.83	-	22.24	0.62
C50	12.53	-	22.66	-	27.63	2.20
C70	15.99	-	27.37	7.10	32.70	12.94
C90	18.48	-	30.97	11.72	37.06	18.54

Figures 14 to 16 show the reliability indices for beams with heights of 40, 50, and 60 centimeters, respectively, calculated using the FORM.

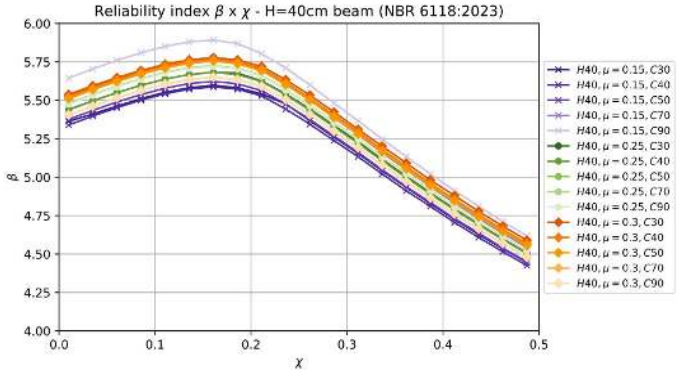


Figure 14 β x χ curves for 40 centimeters height beams designed in accordance with NBR 6118:2023.

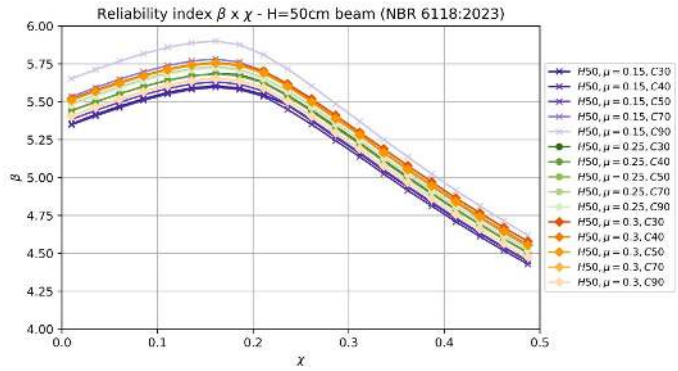


Figure 15 β x χ curves for 50 centimeters height beams designed in accordance with NBR 6118:2023.

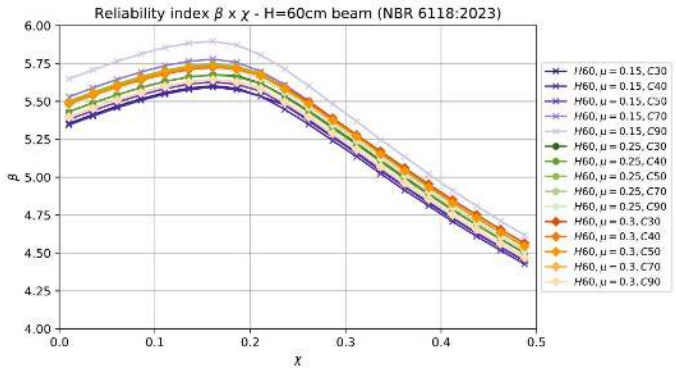


Figure 16 β x χ curves for 60 centimeters height beams designed in accordance with NBR 6118:2023.

Once again, the reliability indices of the three cross-sections showed statistically equivalent results. Also noteworthy were the elements μ = 0.15, C90, which showed an isolated increase in reliability. In a direct comparison with the other elements in the f_{ck} = 90 MPa strength class, the case highlighted had the highest reliability indices for slightly lower neutral axis depth and was the only singly reinforced concrete cross-section of these. Furthermore, there were no significant variations in the directional cosines of the random variables for the elements under discussion.

5.3 Comparative analysis

This section is dedicated to comparing the design and reliability results obtained previously. As noted, the change in the height of the cross-sections did not influence the calculated reliability, so the conclusions drawn for one of the sections will also be valid for the others (the h = 40 cm beam will be used as a reference). In addition, the changes imposed by the update of NBR 6118:2023 will only apply to elements with f_{ck} greater than 40 MPa. Therefore, the graphs of Figures 17, 18, and 19 are shown, referring to elements with f_{ck} equal to 50, 70, and 90 MPa.

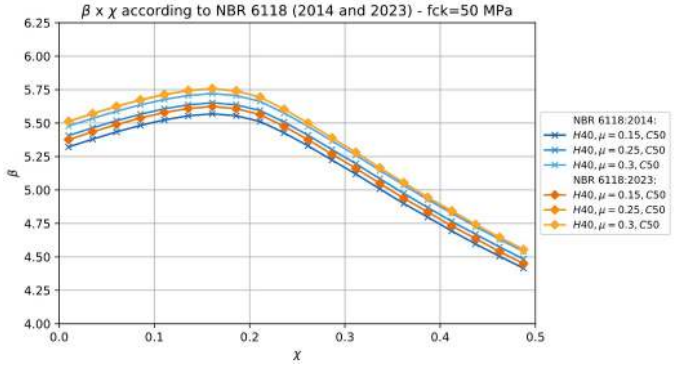


Figure 17 Reliability indices for 40 centimeters height beams (C50) – comparison between versions of NBR 6118.

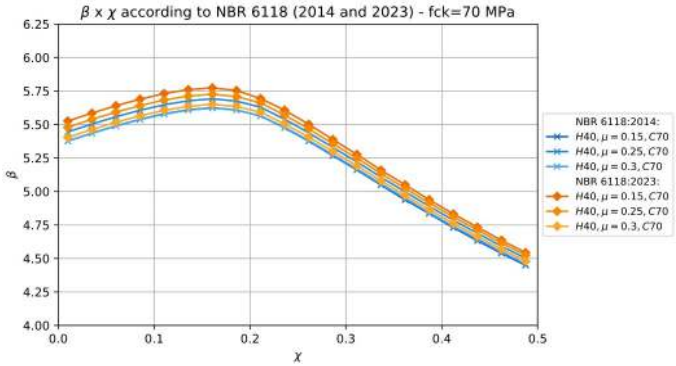


Figure 18 Reliability indices for 40 centimeters height beams (C70) – comparison between versions of NBR 6118.

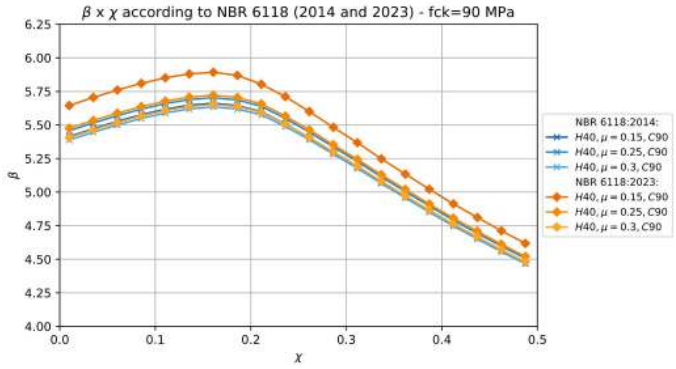


Figure 19 Reliability indices for 40 centimeters height beams (C90) – comparison between versions of NBR 6118.

Firstly, it should be noted that the target recommended reliability index by the *fib* Model Code 2010 for buildings with moderate failure consequences over a 50-year period ($\beta \geq 3.80$) was exceeded in all the cases simulated by both versions of the Brazilian code.

In general, despite the changes introduced in the 2023 update of NBR 6118, only minor changes were observed in the reliability indices of beams subjected to simple bending. For C90, where the strength reduction factor has its lowest (most conservative) value, and for the reduced moment 0.15, where the height of the compressed zone of the concrete section is minimal, the assumptions of NBR 6118:2023 lead to a higher value of the reliability index. Table 9 below provides a comparative summary of design and reliability variations according to the two latest versions of the Brazilian code.

Table 9 Summary of design and reliability variations for h = 40 cm cross-sections

Cross-section	$A_{s,total_{2023}}$ / $A_{s,total_{2014}}$	$\beta_{max,2023}$ / $\beta_{max,2014}$
H40, μ = 0.15, C50	1.008	1.010
H40, μ = 0.15, C70	1.021	1.026
H40, μ = 0.15, C90	1.032	1.041
H40, μ = 0.25, C50	1.017	1.019
H40, μ = 0.25, C70	1.149	1.006
H40, μ = 0.25, C90	1.193	1.003
H40, μ = 0.30, C50	1.038	1.006
H40, μ = 0.30, C70	1.109	1.005
H40, μ = 0.30, C90	1.142	1.003

As can be seen, there is a tendency for the reliability curves of the elements designed by the 2014 and 2023 versions of the Brazilian code to converge. Even though the steel areas calculated in accordance with the 2023 update exceed the results of the previous version of NBR 6118 by up to 19% (for the extreme cases), the β values showed increments of 4.1% or less, represented in Table 9 by the comparison between the maximum β values of the series.

6 CONCLUSION

This study evaluated and compared the design and reliability results of reinforced concrete cross-sections under simple bending at the ultimate limit state, according to the recommendations of the 2014 and 2023 versions of the Brazilian code NBR 6118. The rectangular cross-sections were checked using a computational mechanical model to estimate the actual strength capacity of the elements. The model employed the recommendations of the *fib* Model Code 2010 (2013) and was validated for a set of 52 flexure test results. The reliability analyses were carried out using the probabilistic models of the random variables shown in Table 2 through the application of the FORM, and the iHRLF algorithm for optimizing the design point approach.

Throughout the analyses, it was noticed that there is a tendency for maximum reliability indices to occur at values of χ of approximately 0.17. After this point, there is a decrease in the β index due to the increase in uncertainties associated with the variable loads. The results showed that there are no statistically significant differences between the reliability indices obtained for three different cross-sections (40, 50, and 60 centimeters high), as long as the dimensionless bending moments and the δ ratio (d'/d=0.10) are constant.

The reliability curves obtained for sections with different loadings and characteristic strengths showed very similar results, with variations of around 3%. This applies to elements designed according to both the 2014 and 2023 versions of NBR 6118. In all cases, the reliability indices have far exceeded the target values $\beta \geq 3.80$ recommended by the *fib* Model Code 2010 (2013) for buildings with moderate failure consequences over a 50-year reference period.

As for the variations observed, it was possible to conclude that the addition of the strength reduction factor (η_c) increased the total steel areas of the cross-sections by up to 19% in sections with a f_{ck} above 40 MPa. However, a direct comparison between the two versions of the Brazilian code showed that the calculated reliability indices suffered a negligible increase, as only a single case presented an increase of 4.1%. Thus, at least for the simple bending cases covered by the study, the increases in steel consumption observed for the cross-sections dimensioned by NBR 6118:2023 are not entirely justified from the perspective of structural reliability.

Finally, based on the procedures and methodologies developed in this study, some suggestions for future work on this line of research can be listed:

- Assess the reliability and impacts of the update of NBR 6118:2023 concerning reinforced concrete columns.
- Based on the computational mechanical models presented, perform a calibration of the partial safety coefficients of NBR 6118 for a fixed target reliability index.
- Conduct a more in-depth study on the variabilities related to geometric parameters of the sections, such as reinforcement covers, aiming for better representation concerning the reality of construction sites.

Acknowledgments

The authors wish to acknowledge the support from the Brazilian governmental research institutions CAPES and CNPQ.

Author's Contribuitions: Methodology, Validation, Formal analysis, Investigation, Writing original draft, GM Machado; Conceptualization, Reviewing and editing, Supervision, Project administration, A Campos Filho e M de Vasconcellos Real.

Editor: Marco L. Bittencourt

References

ABNT (2014). NBR 6118:2014. Projeto de Estruturas de Concreto – Procedimento. Rio de Janeiro, Brazil. ISBN 978-85-07-04941-8.

ABNT (2023). NBR 6118:2023. Projeto de Estruturas de Concreto. Rio de Janeiro, Brazil. ISBN 978-85-07-09632-0.

Ang, A. H., Tang, W. H., (2006). Probability Concepts in Engineering: Emphasis on Applications to Civil and Environmental Engineering, 2nd ed., Wiley (New York). ISBN 978-0471720645.

Araújo, J. M., (2014). Curso de Concreto Armado, 4th ed, vol. 1, Dunas (Rio Grande). ISBN 978-85-86717-14-7.

Arezoumandi, M., Smith, A., Volz, J. S., Khayat, K. H., (2015). An experimental study on flexural strength of reinforced concrete beams with 100% recycled concrete aggregate, Engineering Structures, vol. 88, 2015, 154-162, http://dx.doi.org/10.1016/j.engstruct.2015.01.043.

Base, G. D., Read, J. B., (1965). Effectiveness of helical binding in the compression zone of concrete beams, ACI Journal, vol. 62, no. 7, 1965, 763-782. DOI: 10.14359/7722.

Borges, C. K., (2023). Análise da Introdução do Fator ηc pela NBR 6118:2023 no Dimensionamento de Seções Poligonais de Concreto Armado Submetidas à Flexo-compressão Oblíqua, in Seminário Sul Brasileiro de Pontes e Estruturas, Porto Alegre, Brazil. Available: http://hdl.handle.net/10183/272171.

Bresler, B., Scordelis, A. C., (1963). Shear strength of reinforced concrete beams, ACI Journal, vol. 60, no. 1, 1963, 51-74. DOI: 10.14359/7842.

Canaval, J. H., (2016). Estudo experimental do comportamento de vigas de concreto armado reforçadas à flexão por meio de graute, armaduras e conectores, M.Sc. Thesis (in Portuguese), Univ. Fed. de Uberlândia, Uberlândia, Brazil, http://doi.org/10.14393/ufu.di.2016.429.

CEN (2004). EN 1992-1-1:2004. Eurocode 2: Design of Concrete Structures: Part 1-1: General Rules and Rules for Buildings. Brussels, Belgium.

Coelho, J. D., (2011). Confiabilidade de vigas de concreto armado no estado limite de serviço, Ph.D. Thesis (in Portuguese), Univ. Federal de Santa Catarina, Florianópolis, Brazil. Available: http://repositorio.ufsc.br/xmlui/handle/123456789/95593.

fib (2010). Model Code for Concrete Structures 2010, Ernst & Sohn, Berlin, Germany.

Garcia, S. L. G., (2018). Taxa de Armadura Transversal Mínima em Vigas de Concreto Armado, Ph.D. Thesis (in Portuguese), COPPE, Univ. Federal do Rio de Janeiro, Rio de Janeiro, Brazil. Available: http://www.coc.ufrj.br/pt/teses-de-doutorado/146-2002/936-sergio-luis-gonzalez-garcia.

Haldar, A., Mahadevan, S., (2000). Probability, Reliability, and Statistical Methods in Engineering Design, John Wiley & Sons (New York). ISBN: 978-0-471-33119-3.

Janney, J. R., Hognestad, E., McHenry, D., (1956). Ultimate flexural strength of prestressed and conventionally reinforced concrete beams, ACI journal, vol. 52, no. 2, 1956, 605-620. DOI: 10.14359/11618.

JCSS (2001a). Probabilistic Model Code: Part 1 – Basis of Design. Accessed: June, 22, 2023. [Online]. Available: https://www.jcss-lc.org/jcss-probabilistic-model-code/.

JCSS (2001b). Probabilistic Model Code: Part 3 - Resistance models. Accessed: June, 22, 2023. [Online]. Available: https://www.jcss-lc.org/jcss-probabilistic-model-code/.

Kong, P. Y. L., Rangan, B. V., (1998). Shear strength of high-performance concrete beams, ACI Journal, vol 95, no. 6, 1998, 705-715. DOI: 10.14359/581.

Kulkarni, S. M., Shah, S. P., (1998). Response of reinforced concrete beams at high strain rates, ACI Journal, vol. 95, no. 6, 1998, 705-715. DOI: 10.14359/584.

Lopes, M. T. A., (2007). Análise de Confiabilidade de Estruturas Aplicada ao Projeto de Reforço à Força Cortante de Vigas em Concreto Armado com Compósitos de Fibras de Carbono, Ph.D. Thesis (in Portuguese), Pontifícia Universidade Católica do Rio de Janeiro, Rio de Janeiro, Brazil. Available: https://bdtd.ibict.br/vufind/Record/PUC_RIO-1_688997252ea1c96c73c72f6e71d72789.

Machado, G. M. (2024), Análise de confiabilidade aplicada a seções de concreto armado submetidas à flexão simples, M.Sc. Thesis (in Portuguese), Prog. Pós-Grad. Eng. Civil, Univ. Fed. Rio Grande do Sul, Porto Alegre, Brazil. Available: http://hdl.handle.net/10183/277054.

Melchers, R. E., Beck, A. T., (2018). Structural Reliability Analysis and Prediction, 3rd ed., John Wiley & Sons (New York). ISBN 978-1119265993.

Ning, X., Ding, Y., Zhang, F., Zhang, Y., (2015). Experimental study and prediction model for flexural behavior of reinforced SCC beam containing steel fibers, Construction and Building Materials, vol. 93, 2015, 644-653, https://doi.org/10.1016/j.conbuildmat.2015.06.024.

Nowak, A. S., Szerszen, M. M., (2003). Calibration of Design Code for Buildings (ACI 318) Part 1: Statistical Models for Resistance, ACI Structural Journal, vol. 100, no. 3, 2003, 377-382. DOI: 10.14359/12613.

Pires, R. M., Gomes, H. M., (2024). Reliability analysis of simply supported R.C. beam cross-sections in a fire situation according to Brazilian standards, Rev. IBRACON Estrut. Mater., vol. 17, no. 4, e17403, 2024, https://doi.org/10.1590/S1983-41952024000400003.

Prieto Rabade, M., Tanner, P., (2008). Incertidumbres del modelo de resistencia a flexión para vigas con armaduras corroídas, in Congreso de ACHE, Valencia, Spain. Available: https://www.researchgate.net/publication/282851145_Incertidumbres_del_modelo_de_resistencia_a_flexion_para_vigas_con_armaduras_corroidas.

Ribeiro, K., Loriggio, D. D., Real, M. de V., (2021). Reliability analysis of very slender columns subjected to creep. Latin American Journal of Solids and Structures, 18(7), e401. https://doi.org/10.1590/1679-78256569.

Santiago, W. C., (2018). Calibração baseada em confiabilidade dos coeficientes parciais de segurança das principais normas brasileiras de projeto estrutural, Ph.D. Thesis (in Portuguese), Prog. Pós-Grad. Eng. Civil, Univ. São Paulo, São Carlos, Brazil, https://doi.org/10.11606/T.18.2019.tde-03042019-092619.

Santiago, W. C., Kroetz, H. M., Beck, A. T., (2019). Reliability-based calibration of Brazilian structural design codes used in the design of concrete structures, Rev. IBRACON Estrut. Mater., vol. 12, no. 6, 1288–1304, Dec. 2019. https://doi.org/10.1590/S1983-41952019000600004.

Santos, D. M., Stucchi, F. R., Beck, A. T., (2014). Reliability of beams designed in accordance with Brazilian codes, Rev. IBRACON Estrut. Mater., vol. 7, no. 5, 723–746, Feb. 2014. https://doi.org/10.1590/S1983-41952014000500002.

Scherer, M., Titello, E. P., Morsch, I. B., Real, M. de V., Campos Filho, A., (2021). Comparison of two FORM methodologies for reinforced concrete beams under flexure. Latin American Journal of Solids and Structures, 18(7), e402. https://doi.org/10.1590/1679-78256670.

Schuler, L., (2023). Estudo Comparativo do Dimensionamento de Pilares de Concreto Armado de Acordo com a NBR 6118:2014 e a NBR 6118:2023, in Seminário Sul Brasileiro de Pontes e Estruturas, Porto Alegre, Brazil. ISBN 978-65-994281-1-1.

Stewart, M. G., (1996). Serviceability Reliability Analysis of Reinforced Concrete Structures, Journal of Struct. Engin., 1996, vol 122, no. 7, 794-803, https://doi.org/10.1061/(ASCE)0733-9445(1996)122:7(794).

Stucchi, F. R., Santos, S. H. C., (2007). Reliability based comparison between ACI 318-05 and NBR 6118, Rev. IBRACON Estrut., vol. 3, no.2, 230–239. Available: https://ibracon.org.br/publicacoes/revistas_ibracon/rev_estruturas/pdf/Riest_-_vol3_-_n_2_-_artigo_5_-_ingles.pdf.

Stucchi, F. R., Santos, S. H. C., Franco, R. M., (2011). Evaluation of the safety criteria of Brazilian Standard NBR 6118 for slender members based on reliability analyses, Applic. of Statistics and Probab. in Civil Engin., 2011, 2761-2767, http://hdl.handle.net/11449/194814.